*Aging Cell* (2013) **12**, pp292–302 Doi: 10.1111/acel.12054

# $Ca^{2+}$-dependent endoplasmic reticulum stress correlates with astrogliosis in oligomeric amyloid β-treated astrocytes and in a model of Alzheimer's disease

Elena Alberdi,[1,2] Ane Wyssenbach,[1,2] María Alberdi,[1,2] Mª V. Sánchez-Gómez,[1,2] Fabio Cavaliere,[1,2] José J. Rodríguez,[1] Alexei Verkhratsky[1,3] and Carlos Matute[1,2]

[1]Departamento de Neurociencias, Achucarro Basque Center for Neuroscience, Universidad del País Vasco (UPV/EHU),
[2]CIBERNED, Universidad del País Vasco, 48940, Leioa, Spain
[3]Faculty of Life Sciences, The University of Manchester, Manchester, UK

## Summary

**Neurotoxic effects of amyloid β peptides are mediated through deregulation of intracellular $Ca^{2+}$ homeostasis and signaling, but relatively little is known about amyloid β modulation of $Ca^{2+}$ homeostasis and its pathological influence on glia. Here, we found that amyloid β oligomers caused a cytoplasmic $Ca^{2+}$ increase in cultured astrocytes, which was reduced by inhibitors of PLC and ER $Ca^{2+}$ release. Furthermore, amyloid β peptides triggered increased expression of glial fibrillary acidic protein (GFAP), as well as oxidative and ER stress, as indicated by eIF2α phosphorylation and overexpression of chaperone GRP78. These effects were decreased by ryanodine and 2APB, inhibitors of ryanodine receptors and $InsP_3$ receptors, respectively, in both primary cultured astrocytes and organotypic cultures of hippocampus and entorhinal cortex. Importantly, intracerebroventricular injection of amyloid β oligomers triggered overexpression of GFAP and GRP78 in astrocytes of the hippocampal dentate gyrus. These data were validated in a triple-transgenic mouse model of Alzheimer's disease (AD). Overexpression of GFAP and GRP78 in the hippocampal astrocytes correlated with the amyloid β oligomer load in 12-month-old mice, suggesting that this parameter drives astrocytic ER stress and astrogliosis *in vivo*. Together, these results provide evidence that amyloid β oligomers disrupt ER $Ca^{2+}$ homeostasis, which induces ER stress that leads to astrogliosis; this mechanism may be relevant to AD pathophysiology.**

**Key words: astroglia; amyloid β; $Ca^{2+}$ dysregulation; ER stress; Alzheimer's disease.**

## Introduction

Alzheimer's disease (AD) is a neurodegenerative disorder characterized by progressive neurodegeneration, intra- and extracellular deposition of amyloid β peptide and formation of neurofibrillary tangles in the brain (Selkoe, 2001). However, it has been difficult to determine which of the amyloid β forms induces the neuropathological changes prominent for the disease. Oligomers have been found in mouse models of AD (Oddo *et al.*, 2006; Tomiyama *et al.*, 2010), as well as in the cerebrospinal fluid and brain tissue (Bao *et al.*, 2012) of patients with AD. The concentrations of soluble amyloid β species apparently correlate with the disease progression (Santos *et al.*, 2012). In neurons, amyloid β oligomers alter $Ca^{2+}$ homeostasis and cause synaptic loss, hyperexcitability, and excitotoxicity (De Felice *et al.*, 2007; Shankar *et al.*, 2007; Busche *et al.*, 2008; Kuchibhotla *et al.*, 2008; Alberdi *et al.*, 2010).

The role of astrocytes and the mechanisms that implicate them in the pathophysiology of AD remain poorly understood. It has been suggested that dysregulation of astrocyte intracellular calcium ($[Ca^{2+}]_i$) homeostasis contributes to AD pathophysiology. Exposure of cultured astrocytes to amyloid $\beta_{1\text{-}42}$ triggered transient elevations in $[Ca^{2+}]_i$ associated with $Ca^{2+}$-dependent glutathione depletion and the formation of reactive oxygen species (ROS), causing astrocytic metabolic failure that may directly inflict neuronal cell death (Abramov *et al.*, 2003, 2004; Abeti *et al.*, 2011). Notably, spontaneous intercellular $Ca^{2+}$ waves independent of neuronal hyperactivity have been identified in astrocytes *in vivo* in APP/PS1 mice (Kuchibhotla *et al.*, 2009). Additionally, reactive astrogliosis, characterized by upregulation of glial fibrillary acidic protein (GFAP), is associated with amyloid plaques and neurofibrillary tangles in AD (Olabarria *et al.*, 2010).

Here, we examined the effects of soluble amyloid $\beta_{1\text{-}42}$ oligomers on astrocyte biology. We studied cultured astrocytes, slices of the entorhinal cortex and hippocampus, and brain tissues obtained from intracerebroventricularly amyloid β-injected rats and from the 3 × Tg-AD mouse model (Oddo *et al.*, 2003) that carries transgenes encoding mutants of presenilin-1 (PS1; M146V), amyloid precursor protein (APP; swe), and tau (P301L). Our results indicate that amyloid $\beta_{1\text{-}42}$ oligomers altered endoplasmic reticulum (ER) $Ca^{2+}$ homeostasis by inducing $Ca^{2+}$ release through ryanodine receptors (RyRs) and $InsP_3$ receptors ($InsP_3Rs$). This ultimately resulted in activation of oxidative and ER stress and astrogliosis, which was assessed *in vitro* and *in vivo* in astrocytes exposed to amyloid β oligomers. Furthermore, amyloid β levels correlated with the molecular changes in ER and astrocytic physiology observed in the hippocampi of transgenic mice with a brain condition that models AD.

## Results

### Amyloid β oligomers raise $[Ca^{2+}]_i$ by stimulating $Ca^{2+}$ release from the ER in astrocytes

Previous studies have shown changes in astroglial $[Ca^{2+}]_i$ caused by different preparations of amyloid β peptides (1–40, 1–42, and 25–35) with aggregation states not well defined. Some reported that exposure of cultured astrocytes to amyloid β increases $[Ca^{2+}]_i$ (Stix & Reiser, 1998; Abramov *et al.*, 2003; Chow *et al.*, 2010),

Correspondence
*Carlos Matute, Departamento de Neurociencias, Universidad del País Vasco, E-48940 Leioa, Spain. Tel.: +34-94-601-3244; fax: +34-94-601-3400; e-mail: carlos.matute@ehu.es*

Accepted for publication *02 February 2013*

whereas others found $[Ca^{2+}]_i$ decreases (Meske *et al.*, 1998). Based in our previous results in neurons (Alberdi *et al.*, 2010), we explored the effects of soluble amyloid $\beta_{1-42}$ oligomers at 5 μM on $[Ca^{2+}]_i$ in cultured astrocytes (Fig. 1H, lane 3). Immediately after application of the peptide, fluorescent $Ca^{2+}$ imaging showed increased $[Ca^{2+}]_i$ in the cultured astrocytes. Responsive cells showed a complex signaling patterns, which included large spikes of variable frequency that lasted several minutes; this was followed by sustained elevation in $[Ca^{2+}]_i$ (Fig. 1A,G). No $Ca^{2+}$ responses were observed when unaggregated amyloid $\beta_{1-40}$ peptide (data not shown) or fibrillar amyloid $\beta_{1-42}$ (Fig. 1E,H, *lane 2*) was applied to cultured astrocytes. To rule out the possibility that $[Ca^{2+}]_i$ changes result from astrocyte damage, we measured cell viability after peptide treatment by calcein assay and found no toxicity (Fig 1F).

The rise of $[Ca^{2+}]$ could originate from $Ca^{2+}$ influx through the plasma membrane, from the release of $Ca^{2+}$ from an internal stores or a combination of both. To explore these possibilities, we examined the responses in a $Ca^{2+}$-free extracellular buffer that contained 50 μM EGTA (Fig. 1B). Under these conditions, oligomeric amyloid β produced the initial spikes of $Ca^{2+}$ but not the late sustained $Ca^{2+}$ response seen when $Ca^{2+}$ is present in the medium indicating a primary role for $Ca^{2+}$ release from the intracellular $Ca^{2+}$ stores and a later $Ca^{2+}$ contribution through extracellular $Ca^{2+}$ influx. The oscillatory profile shape of $[Ca^{2+}]_i$ signals revealed by amyloid β application were qualitatively similar and characteristic to the $InsP_3$-triggered intracellular $[Ca^{2+}]_i$ release, as previously described for astrocytes (Peuchen *et al.*, 1996; Verkhratsky & Kettenmann, 1996). Therefore, we investigated whether amyloid β peptides could activate phospholipase C (PLC), which generates $InsP_3$ that subsequently mobilizes ER $Ca^{2+}$. Figures 1C and G show that $InsP_3R$ and PLC inhibitors, 2APB (10 μM) and U73122 (5 μM), respectively, blocked totally the $Ca^{2+}$ increase in amyloid β-treated astrocytes. These results indicate that $InsP_3R$ activation contributes to $Ca^{2+}$ spikes and modulates late sustained $Ca^{2+}$ increase. Release of $Ca^{2+}$ by RyRs is normally triggered by elevated cytosolic $Ca^{2+}$ ($Ca^{2+}$-induced $Ca^{2+}$ release). The expression and role of RyRs in astrocytes are controversial (for review, see Fiacco & McCarthy, 2006); therefore, we tested the specific contribution of RyRs to amyloid β-induced $Ca^{2+}$ increases. An antagonistic concentration of ryanodine (50 μM) led to a reduced amyloid β-induced primary $Ca^{2+}$ response in astrocytes but did not modify the sustained elevation in $[Ca^{2+}]_i$, indicating that $Ca^{2+}$ release by RyR is a primary component in the amyloid β-induced $Ca^{2+}$ signals (Fig. 1D,G).

As follow-up of these initial data showing an amyloid β-dependent PLC activation and of previous results in neurons (Alberdi *et al.*, 2010), we investigated whether the $[Ca^{2+}]_i$ increases were dependent on metabotropic and/or ionotropic glutamate or purinergic receptor activation. We measured amyloid β-induced $Ca^{2+}$ levels in presence of LY367385 (100 μM) and SIB1757 (10 μM), selective antagonists of mGluR1 and mGluR5, respectively, AP5 (100 μM) antagonist of NMDA receptors, CNQX (30 μM) antagonist of AMPA/kainate receptors and PPADS (100 μM) antagonist of purinergic P2 receptors. $Ca^{2+}$ recordings showed that none of analyzed drugs altered the amyloid β-induced $Ca^{2+}$ signals in astrocytes (Fig 1G). Taken together, these results indicate that release of $Ca^{2+}$ stored in the ER and extracellular $Ca^{2+}$ influx underlie amyloid β-induced $[Ca^{2+}]_i$ signaling.

### Amyloid β-induced GFAP upregulation is attenuated by inhibitors of ER-$Ca^{2+}$ release

Previous studies showed that treatment with amyloid $\beta_{1-42}$ oligomers increases the immunoreactivity for astrocyte intermediate filaments and GFAP in cultured astrocytes (Garwood *et al.*, 2011). Here, we examined whether the increase in astrocyte GFAP expression was dependent on amyloid β-induced intracellular $Ca^{2+}$ changes. Immunolocalization of GFAP revealed that oligomeric amyloid β (5 μM, 24 h) affected the morphology of astrocytes inducing typical astrogliotic characteristics, including hypertrophy and increased branching (Fig. 2A). Furthermore, Western blot quantification of astrocyte protein samples showed that amyloid β-treatment upregulated GFAP levels in a concentration-dependent manner, with maximal activation achieved at approximately 2.5–5 μM (Fig. 2B). To determine whether amyloid β-induced intracellular $Ca^{2+}$ changes modified GFAP levels, we treated astrocytes with peptide (5 μM, 24 h) in the presence of 2APB (10 μM) or ryanodine (50 μM) and quantified the GFAP levels on Western blots. Peptide treatment upregulated GFAP expression by 128 ± 3.7% ($n$ = 8 cultures) compared with untreated cells (100%), and this response was completely blocked by co-treatment with 2APB (95 ± 7% compared with cells treated only with 2APB, $n$ = 8 cultures) or with ryanodine (89 ± 9%, compared with cells treated only with ryanodine, $n$ = 4; Fig. 2C).

We next examined effect of chronic treatment (4 days) with amyloid β oligomers (100 nM) on ER $Ca^{2+}$-dependent GFAP overexpression in a brain slice preparation. We tested organotypic cultures of the entorhinal cortex and hippocampus, two regions that are profoundly affected in AD. Slices were prepared to preserve the major connections between the entorhinal cortex and hippocampus (Alberdi *et al.*, 2010). Organotypic slices were chronically incubated with low concentrations of amyloid β oligomers (100 nM, 4 days) alone or together with 2APB (10 μM) or ryanodine (50 μM). Changes in GFAP were quantified by fluorimetry (Fig. 2D). Slices showed increased GFAP levels of 147 ± 10% ($n$ = 6 cultures), compared with untreated slices (100%). This response was completely blocked by 2APB (99 ± 9% compared with slices treated only with 2APB, $n$ = 6 cultures) and significantly reduced by ryanodine (113 ± 9% compared with slices treated only with ryanodine, $n$ = 6 cultures).

Overall, these results indicate that amyloid β oligomers upregulated GFAP expression in an ER $Ca^{2+}$ release-dependent manner in cultured astrocytes and organotypic slices.

### Amyloid β oligomers cause RyR- and $IP_3R$-dependent ER stress in astrocytes and ROS generation

Disturbance of ER $Ca^{2+}$ homeostasis may perturb ER functions, induce ER stress, and, consequently, cause cell death (Verkhratsky & Petersen, 2002). The ER stress, can develop in several ways, which often include the unfolded protein response (UPR). The ER stress also shuts down general protein synthesis and upregulates some $Ca^{2+}$ homeostasis-related proteins (e.g., chaperones). Several recent reports have described activation of UPR in the neurons from AD

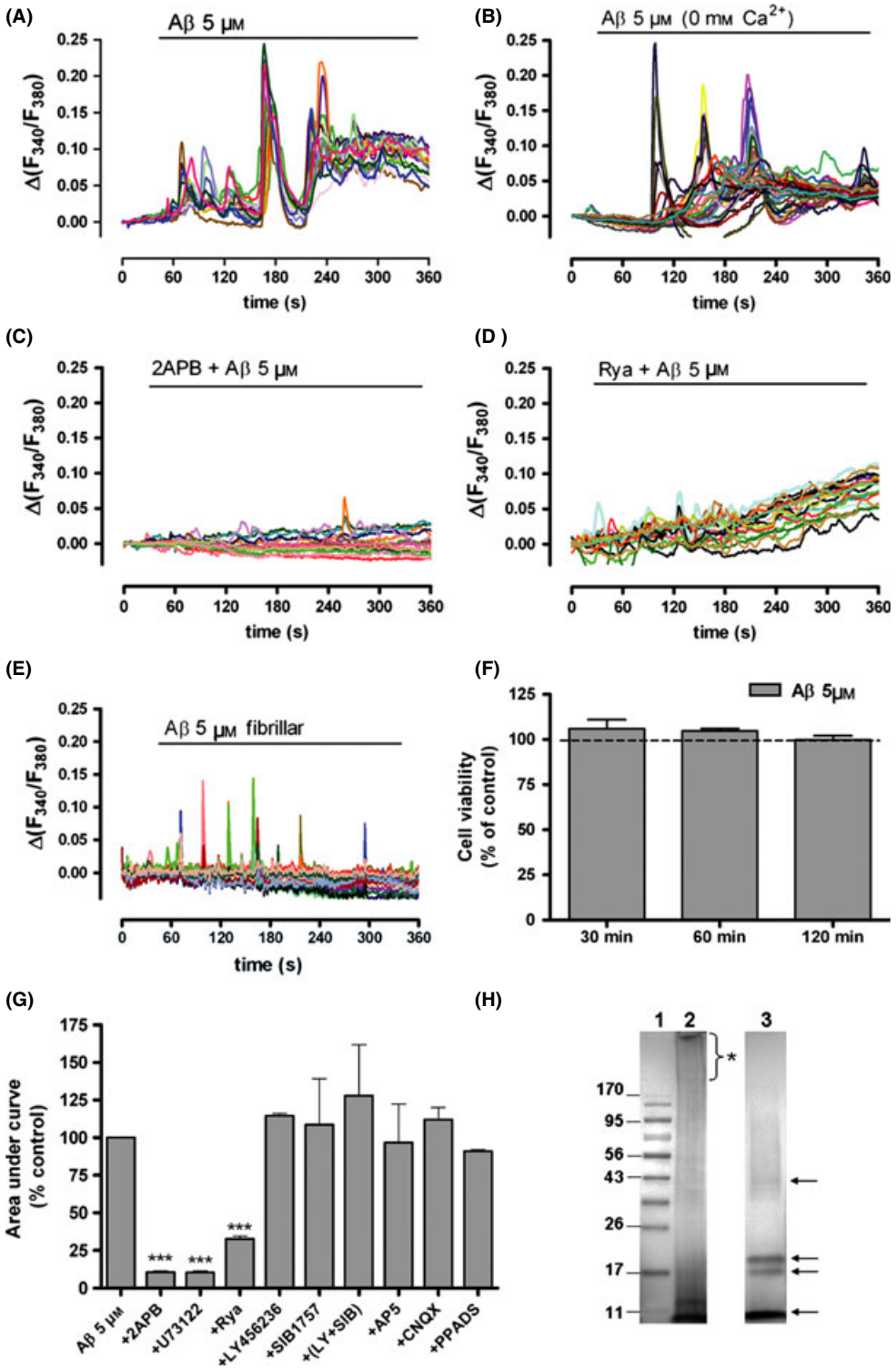


**Fig. 1** Aβ oligomers increase $[Ca^{2+}]_i$ in rat astrocytes. Cells were exposed to Aβ oligomers and $Ca^{2+}$ levels were measured in (A) $Ca^{2+}$-containing extracellular buffer, (B) $Ca^{2+}$-free extracellular buffer plus EGTA (50 μM) (C) in the presence of the $IP_3R$ inhibitor 2APB (10 μM) (D) or the RyR inhibitor ryanodine (Rya; 50 μM). (E) Astrocyte $Ca^{2+}$ recordings produced by Aβ fibrillar 5 μM are shown. (F) Bars represent the mean ± SEM of astrocyte viability measured by calcein assay and expressed as a percentage of untreated cells (100%). (G) Bars represent the mean ± SEM of $Ca^{2+}$ increases, quantified as the area under the curve in treated astrocytes and expressed as a percentage of the level in Aβ-exposed cells (100%). $^{**}P < 0.001$ as compared to Aβ-treated samples. (H) Representative Western blot showing broad range molecular weight protein markers (lane 1), fibrillar (lane 2), and oligomeric (lane 3) preparation of amyloid $\beta_{(1\text{-}42)}$ probed with monoclonal antibody 6E10. Asterisk indicates large aggregates of more than 170 kDa in fibrillar preparation and arrows show monomers and major components migrating at ~18 kDa in addition to a higher molecular weight band in oligomeric preparation.

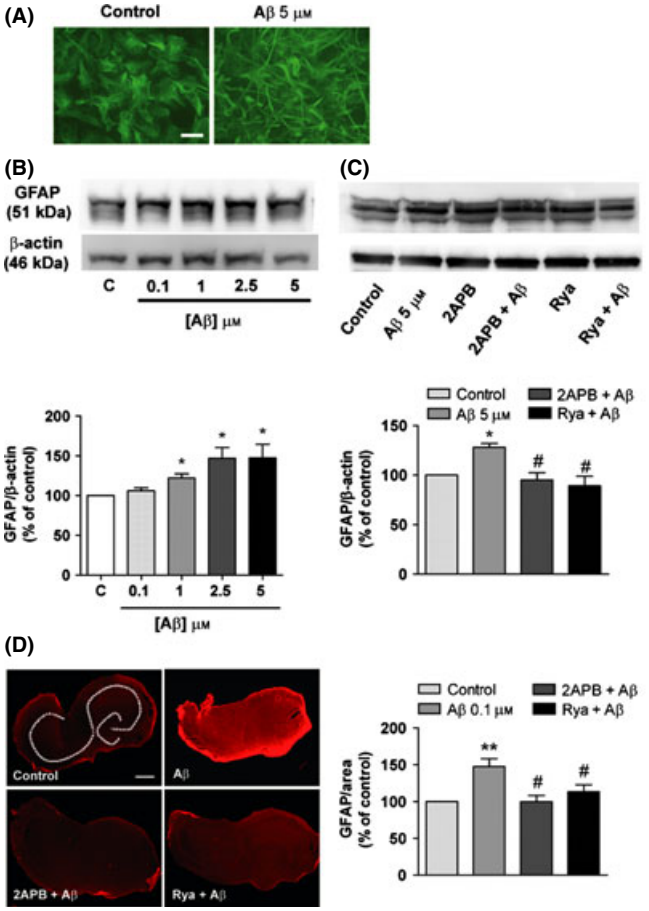


**Fig. 2** Inhibitors of ER $Ca^{2+}$ release attenuate Aβ-induced GFAP upregulation in cultured astrocytes and in entorhinal cortex-hippocampus organotypic cultures. (A and B) Photographs show immunocytochemistry and Western blot analysis of astrocytic GFAP after Aβ treatment for 24 h. Data represent the mean ± SEM of GFAP optical density normalized to β-actin values for $n = 4$ cultures. (C) Western blot analysis of GFAP after Aβ-treatment (5 μM) with or without ER $Ca^{2+}$ inhibitors for 24 h. Data represent the mean ± SEM of GFAP optical density normalized to β-actin values; $n = 8$ cultures. (D) Photographs show immunolabeled GFAP (red) in organotypic slices after Aβ treatment (100 nM, 4 days) with or without ER $Ca^{2+}$ release inhibitors (left; bar = 100 μm). Histogram shows the mean ± SEM of GFAP signal per slice area, expressed as a percentage of the signal detected in control, untreated slices (100%) (right: $n = 6$ cultures). $^{*}P < 0.05$, $^{**}P < 0.01$ compared with untreated control; $^{\#}P < 0.05$, compared with Aβ-treated samples.

brains (Hoozemans *et al.*, 2009; Scheper *et al.*, 2011), and induction of mild ER stress in neuronal cells following exposure to amyloid $\beta_{1-42}$ peptides (Chafekar *et al.*, 2007). However, there is no evidence for UPR activation in glial cells in brains of patients with AD. We investigated whether amyloid β oligomers induced ER stress in astrocytes and whether this response involved changes in ER $Ca^{2+}$ levels induced by release through RyRs and/or $InsP_3Rs$. We quantified two ER stress markers: (i) the downstream target of the ER stress sensor pPERK phosphorylated and total eIF2α (peIF2α and eIF2α) and (ii) the chaperone GRP78 (BIP). We found that amyloid β oligomers (5 μM, 1 h) triggered an increase in peIF2α (132 ± 13%, $n = 4$) compared with untreated cells (100%). This response was reduced significantly by 2APB (122 ± 10%, $n = 4$), and completely blocked by ryanodine (93 ± 3%, $n = 4$; Fig. 3A). 2APB and ryanodine did not significantly increase the eIF2α total protein level (115 ± 24%; and 107 ± 22%, $n = 4$, as compared to β-actin levels) excluding an alternative mechanism for eIF2α phosphorylation. Peptide treatment (5 μM, 6 h) also upregulated GRP78 expression to 151 ± 12% ($n = 8$); this response was abolished by both 2APB and ryanodine (100 ± 8 and 72 ± 6%, respectively, $n = 8$ each; Fig. 3A).

Previous reports have shown that amyloid β peptides increase ROS production in $Ca^{2+}$-dependent manner in neurons (De Felice *et al.*, 2007; Alberdi *et al.*, 2010) and astrocytes (Abramov *et al.*, 2004). To determine whether ER $Ca^{2+}$ contributed to amyloid β-induced ROS production in astrocytes, we used CM-DCFDA, which is oxidized to a fluorescent product by ROS, in such a manner that the rate of increase in the signal indicates the rate of ROS generation. After 30 min of amyloid β oligomer treatment (5 μM), we detected a rapid transient increase in the DCF signal (137 ± 6% compared with 100% in untreated cells, $n = 4$). After 60 and 120 min of treatment, the signal was reduced to 125 ± 14 and 113 ± 7% ($n = 4$), respectively (Fig. 3B). ROS production at 30 min was almost completely inhibited by ryanodine (50 μM; 106 ± 2%, $n = 4$) and thapsigargin (1 μM; 108 ± 3%, $n = 4$). 2APB treatment caused a statistically nonsignificant increase of amyloid β-stimulated ROS generation (153 ± 24%, $n = 4$; Fig. 3C). Taken together, these data demonstrate that RyR- and $IP_3R$-dependent $Ca^{2+}$ release from the ER contributes to amyloid β-induced ER stress, whereas only $Ca^{2+}$ release via RyRs triggers oxidative stress in astrocytes.

### Amyloid β oligomers promote $Ca^{2+}$-dependent ER stress in astrocytes of organotypic slices

We next examined whether a $Ca^{2+}$-dependent UPR occurred in astrocytes and correlated with astrogliosis in organotypic cultures of the entorhinal cortex and hippocampus that were treated with amyloid β oligomers (100 nM; 4 days). Western blot analysis showed significant increases in GFAP (139 ± 14%, $n = 4$) and GRP78 (184 ± 38%, $n = 4$) protein levels compared with control slices (100%, $n = 4$). These effects were blocked by incubation of amyloid β-treated slices with intracellular $Ca^{2+}$ channel blockers 2APB and ryanodine (Fig. 4A,B). Correlation analysis of GRP78 and GFAP expressions showed a significant positive correlation between these two protein levels in treated organotypic slices ($r = 0.631$; $P = 0.0138$; Fig. 4C).

To assess whether ER stress occurred in astrocytes, we used immunofluorescence to analyze GRP78 levels in astrocytes labeled with S100B in amyloid β-treated organotypic slices. Quantification of colocalized fluorescent signals of GRP78 and S100 (Fig. 4D,E) showed that amyloid β oligomer-treated astrocytes expressed higher levels of GRP78 (304.7 ± 41.4%, $n = 4$) compared with control (100%, $n = 7$). Treatment with 2APB and ryanodine reduced GRP78 expression to control levels (107.8 ± 25.8 and 98.5 ± 49.7% $n = 7$, respectively). These results indicate that the $Ca^{2+}$-dependent ER stress is a critical mechanism that mediates astrogliosis in amyloid β-treated astrocytes in organotypic slices.

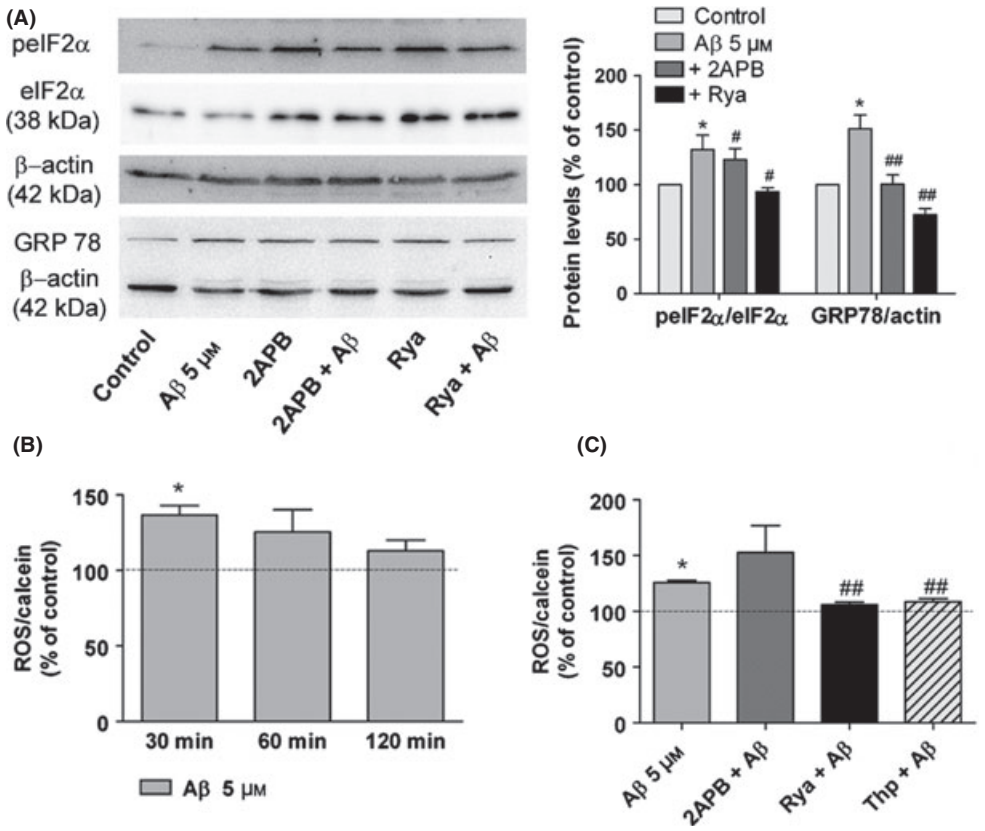


**Fig. 3** 2APB and Rya decrease Aβ-induced ER and oxidative stress in astrocytes. (A) Cells were treated with Aβ oligomers for 1 h (peIF2α) or 6 h (GRP78) in the presence or absence of 2APB (10 μM) or Rya (50 μM). Data represent optical density values normalized to total eIF2α or β-actin values and expressed as a percentage of the control (untreated or 2APB-Rya-treated signal, 100%) ($n = 4$). (B) Astrocytes were treated with Aβ for 30, 60, or 120 min, and ROS generation was monitored with CM-H2DCFDA (30 μM). (C) Rya (50 μM), but not 2APB (10 μM), reduced Aβ-induced ROS generation in astrocytes. Data represent mean ± SEM of the CM-H2DCFDA/calcein signal in $n = 8$ cultures, expressed as a percentage of the control untreated levels (100%). $^{*}P < 0.05$ compared with untreated cells; $^{\#}P < 0.05$, $^{\#\#}P < 0.01$ compared with Aβ-treated cells.

### Acute intracerebroventricular injection of amyloid β oligomers induced GFAP and GRP78 overexpression in astrocytes of dentate gyrus of rat brains

To determine whether the amyloid β-dependent ER stress and astrogliosis found in cell and organotypic culture experiments also occur *in vivo*, we investigated effects of amyloid β oligomers on GFAP and GRP78 expressions in the brains of adult rats. Rats received a single intracerebroventricular (i.c.v.) injection of amyloid β oligomers (40 μg/rat) or vehicle and were sacrificed 3 and 14 days later. To quantify GFAP and GRP78 expressions in hippocampal astrocytes, we used immunolabeling and measured the area positive for GFAP and GRP78 antibodies versus total analyzed area. No significant changes were found in 3 days after injection ($n = 4$; Fig. 5D); however, in 2 weeks after injection, we detected a significant increase of astrocytic GFAP levels (138 ± 10%, $n = 4$ animals; Fig. 5A–D) in the dentate gyrus compared with vehicle-injected rats (control 100%, $n = 4$). At the same time, levels of GRP78 in astrocytes (Fig. 5B,E) were significantly elevated at both 3 and 14 days after injection (133 ± 14 and 141 ± 14%, respectively, $n = 4$ animals per group) compared with the control-injected rats (100%, $n = 4$). Amyloid β injection decreased nonsignificantly the cell density in dentate gyrus as compared with controls (681 ± 30 and 617 ± 30 cells/$mm^2$, respectively). Thus, there is no apparent contribution of cell number to changes of GFAP and GRP78 expression in the studied areas. We confirmed higher GRP78 expression in astrocytes in amyloid β-treated rat brains by double immunofluorescence labeling with S100B (Fig. 5C). Overall, these histological findings were consistent with those described in cultured astrocytes, demonstrating that amyloid β oligomers initiate ER stress in astrocytes and astrogliosis in the brains of rats, establishing the *in vivo* relevance of our findings in the *in vitro* system.

### Oligomeric amyloid β levels correlate with GFAP and GRP78 levels in 3×Tg mice

Previous reports have demonstrated changes in astroglial morphology in the hippocampi of 3×Tg-AD mice at different ages (Olabarria *et al.*, 2010). By Western blot analysis, we examined whether GFAP upregulation was associated with changes in GRP78 and amyloid β oligomer levels in 3×Tg-AD animals (Fig. 6A,B). In protein extract from hippocampi of 12-month-old 3×Tg-AD mice, GFAP and GRP78 levels were increased to

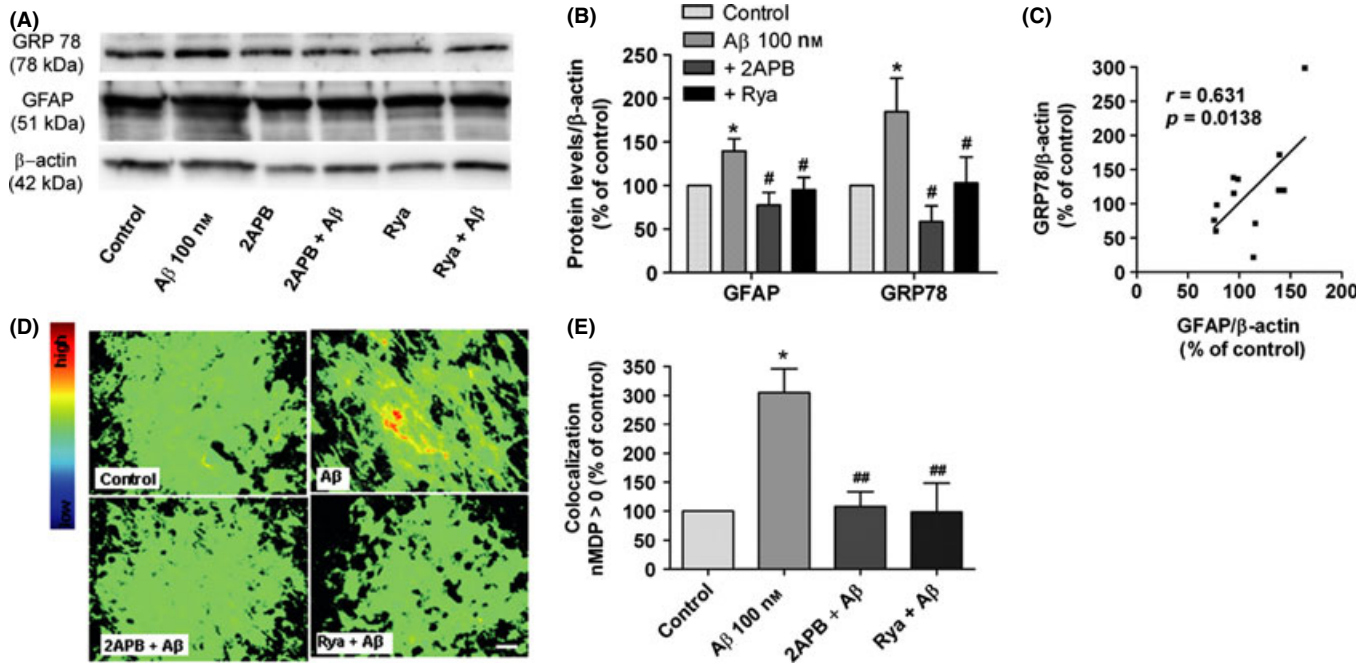


**Fig. 4** $Ca^{2+}$-dependent ER stress in astrocytes in Aβ-treated organotypic slices. (A) Slices were treated with oligomeric Aβ (100 nM, 4 days) in the presence or absence of 2APB (10 μM) or Rya (50 μM). GFAP and GRP78 levels were quantified by Western blot analysis. (B) Data represent optical density values normalized to β-actin values and expressed as a percentage of the control (untreated or 2-APB or Rya-treated slices, 100%). (C) Correlation analyses between GFAP and GRP78 levels in the Aβ-treated slices ($r = 0.631$, $P = 0.0138$, $n = 12$) are shown. (D) Photomicrographs of organotypic slices showing colocalization colormap of intensities of fluorescent signals of GRP78 and S-100-B immunolabeling. Hot colors represent colocalization, whereas cold colors represent exclusion. (E) Colocalization of two markers is expressed as correlation of intensities between pairs of pixel of two different channels. Data represent the normalized mean deviation products >0 of eight photomicrographs of each treatment ($n = 4$ experiments); $^{*}P < 0.05$ compared with untreated cells; $^{\#}P < 0.05$, $^{\#\#}P < 0.01$ compared with Aβ-treated cells.

127 ± 8 and 131 ± 7%, respectively, compared with age-matched non-Tg controls. With the 6E10 antibody, we detected detergent-resistant amyloid β oligomers (pentamers of ~20 kDa) in hippocampal samples of 3×Tg-AD mice (Fig. 6A). Correlation analysis showed a significant positive correlations of GFAP ($r = 0.9756$, $P = 0.0046$) and GRP78 ($r = 0.91$, $P = 0.032$) with hippocampal levels of amyloid β oligomer (Fig. 6C,D). Data analysis also showed a significant positive correlation between GRP78 and GFAP in this AD animal model (Fig. 6E). Overall, these results indicate that overexpression of GFAP and GRP78 is associated with increased levels of amyloid β oligomer in 12-month-old 3×Tg-AD mice. These observations were further corroborated by immunohistochemistry of GFAP and GRP78 in astrocytes. Analysis of the areas of astrocytes labeled with GFAP (Fig. 6F) and GRP78 (Fig. 6G) antibodies versus total area showed increased protein levels in 3×Tg-AD mice (137 ± 18 and 156 ± 15%, respectively) compared with age-matched non-Tg mice (100%). There was no significant changes in astrocyte cell density in 3×Tg-AD as compared with control mice (801 ± 32 and 781 ± 28 cells/mm$^2$, respectively). Double immunofluorescence labeling with the specific astrocytic marker S100B revealed that astrocytes in 3×Tg-AD mice expressed higher GRP78 levels compared with non-Tg mice (Fig. 6H). Overall, these data show that astrogliosis and astrocytic ER stress correlated with increase levels of amyloid β oligomers in the 3×Tg mouse model of AD.

## Discussion

In the present study, we demonstrated that astrocytes responded to the oligomeric form of amyloid β peptide by mobilizing ER $Ca^{2+}$, which triggered ER stress response that initiated astrogliosis. Amyloid β oligomers injected *in vivo* caused a similar response in hippocampal astrocytes, and comparable changes were found in the 3×Tg-AD mice. These results suggest that astrocytic ER stress initiated by amyloid β-dependent $Ca^{2+}$ dysregulation may be directly linked to reactive astrogliosis in AD.

### Oligomeric amyloid β affects astroglial $Ca^{2+}$ homeostasis

Pathogenic interactions between altered cellular $Ca^{2+}$ signaling and amyloid β in its different aggregation states have been extensively described in neurons (for review, see Demuro *et al.*, 2010); however, the effects in astrocytes remain controversial. Here, we found that the $[Ca^{2+}]_i$ rise caused by amyloid $\beta_{1\text{-}42}$ oligomers was due to $Ca^{2+}$ release from intracellular stores, because (i) it occurred in nominally $Ca^{2+}$-free medium and (ii) $[Ca^{2+}]_i$ increases were reduced in the presence of inhibitors of PLC, $InsP_3Rs$, and RyRs. We also show that $Ca^{2+}$ influx contributes to a late sustained $Ca^{2+}$ response that is modulated by $IP_3$ signaling but not by $Ca^{2+}$ release through RyRs. Further experiments will be necessary to define the extracellular $Ca^{2+}$ routes of amyloid β-induced $Ca^{2+}$ response in astrocytes. Consistent with these results, previous observations have also suggested that the

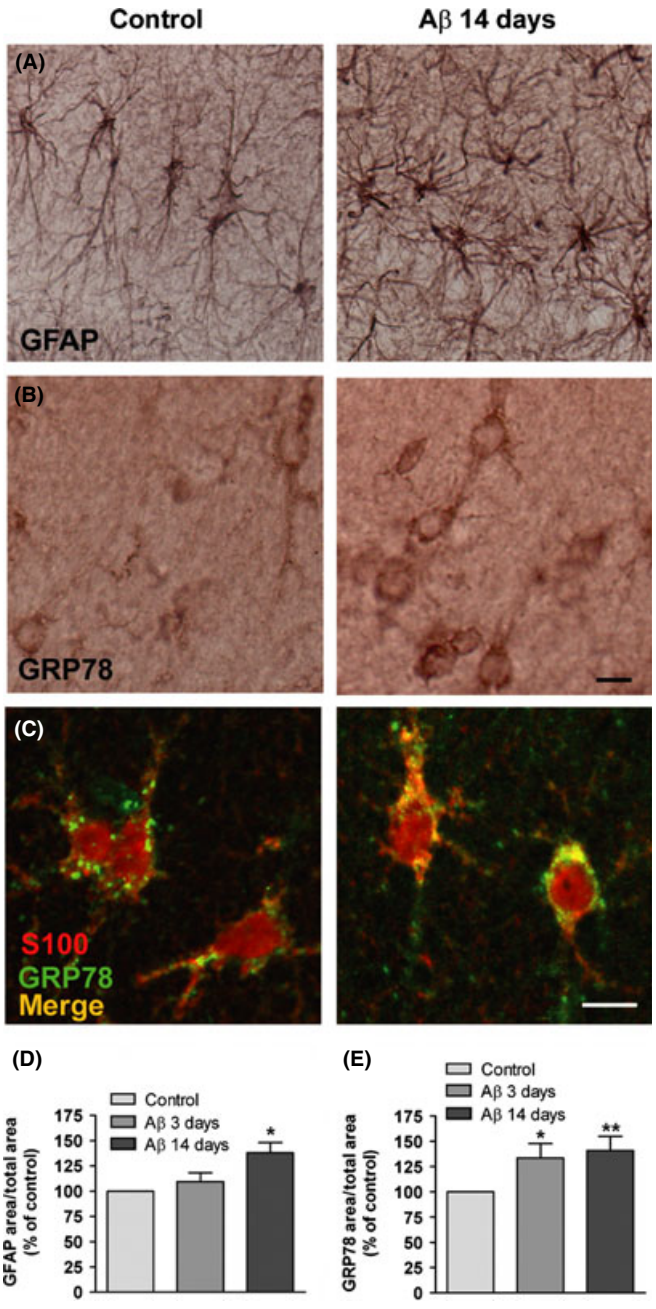


**Fig. 5** Changes in astrocytic levels of GFAP and GFP78 levels after intracerebroventricular injection of Aβ oligomers in rats. Photomicrographs of coronal sections of hippocampi of vehicle- and Aβ-injected (A–D) rats ($n$ = 4 each). The sections ($n$ = 2 for each animal) were processed by immunohistochemistry with anti-GFAP (A) and anti-GRP78 antibodies (B) Bar graphs show the values of the areas labeled for GFAP (D) and GRP78 (E) after 3 and 14 days of Aβ-treatment normalized to control. (C) Photomicrographs of GRP78 protein revealed by double immunofluorescence labeling in S100-$B^+$ rat astrocytes. Bar = 10 μm. *$P$ < 0.05, **$P$ < 0.01 compared with vehicle-injected rats.

neurotoxic fragment of amyloid β (25–35) may activate intracellular $Ca^{2+}$ release (Stix & Reiser, 1998). In contrast, other studies have shown that the full-length amyloid β-induced $Ca^{2+}$ signaling is entirely dependent on $Ca^{2+}$ influx from the extracellular space, through amyloid β inserts into the plasma membrane or by modulating the properties of existing $Ca^{2+}$-permeable channels (Abramov *et al.*, 2003, 2004); however, the source of $Ca^{2+}$ was not precisely defined in these studies. These discrepancies may arise from different stimulation paradigms or different aggregation states of amyloid β peptides. Indeed, our findings indicate that the aggregation states of amyloid β differentially affect $Ca^{2+}$ dysregulation in astrocytes, because only the oligomeric peptide, but not fibrillar and unaggregated amyloid, changes the intracellular $Ca^{2+}$ levels. Similarly, oligomers, but not monomers or fibrils, increased intracellular free $Ca^{2+}$ in neurons (Demuro *et al.*, 2005) and oligomeric, fibrillar and monomeric species differentially affect neuronal viability (Dahlgren *et al.*, 2002). In addition, here we demonstrate that amyloid β-induced $Ca^{2+}$ signaling is dependent on PLC activation, suggesting that amyloid β oligomers could destabilize the membrane leading to PLC translocation (Hicks *et al.*, 2008) or to activation of G protein-coupled receptors. However, selective blockade of metabotropic glutamate or purinergic receptors did not reduce the $Ca^{2+}$ levels reached after amyloid β treatment, indicating that other alternative mechanisms may be involved in this signaling. $Ca^{2+}$ signaling in astrocytes is central to astroglial functions (Araque, 2008); therefore, dysregulation of $Ca^{2+}$ signaling in astrocytes is likely to affect the ability of astrocytes to function as integral components of the nervous system. Dysfunctional astroglial $Ca^{2+}$ signaling is found in many pathological states, including epilepsy, ischemia and cortical spreading depression following stroke or traumatic brain injury (Nedergaard *et al.*, 2010). Functional consequences of disturbed astrocytic $Ca^{2+}$ homeostasis in AD begin to emerge (Vincent *et al.*, 2010). $Ca^{2+}$ signaling is disrupted in astrocytes of transgenic mouse models of AD (Kuchibhotla *et al.*, 2009) and in cultured astrocytes exposed to Aβ peptides (Stix & Reiser, 1998; Abramov *et al.*, 2003; Chow *et al.*, 2010). Collectively, these studies indicate that soluble Aβ is potentially detrimental to astrocytic function.

### Amyloid β oligomers induced $Ca^{2+}$-dependent ER stress in astrocytes

ER stress is involved in neurodegenerative diseases, including AD (Verkhratsky, 2005; Hoozemans *et al.*, 2009). However, molecular mechanisms that underlie amyloid β-induced ER stress and subsequent neurotoxicity remain unknown. In the present study, we demonstrated that amyloid β oligomers induced ER stress in astrocytes *in vitro* and *in vivo*. We observed robust phosphorylation of eIF2α, together with an increased expression of the GRP78 ER-resident chaperones, which are hallmarks of neuronal and glia injury-related UPR (Ruiz *et al.*, 2009, 2010). We additionally showed that ER $Ca^{2+}$ release through RyRs and $InsP_3$Rs was involved in this response; inhibition of both types of receptors diminished eIF2α phosphorylation and the GRP78 increase, most likely by preventing ER $Ca^{2+}$ depletion. These data agree with previous findings in neurons, which showed that oligomeric amyloid β-depleted ER $Ca^{2+}$ and led to intracellular $Ca^{2+}$ dyshomeostasis involving PLC and RyRs (Resende *et al.*, 2008). Moreover, we found that amyloid β-induced oxidative stress in astrocytes was also reduced by inhibitors of RyRs. These data suggest that amyloid β oligomers generate specific cellular stress in astroglia, which is dependent on ER $Ca^{2+}$ homeostasis, similar to previous findings in neurons.

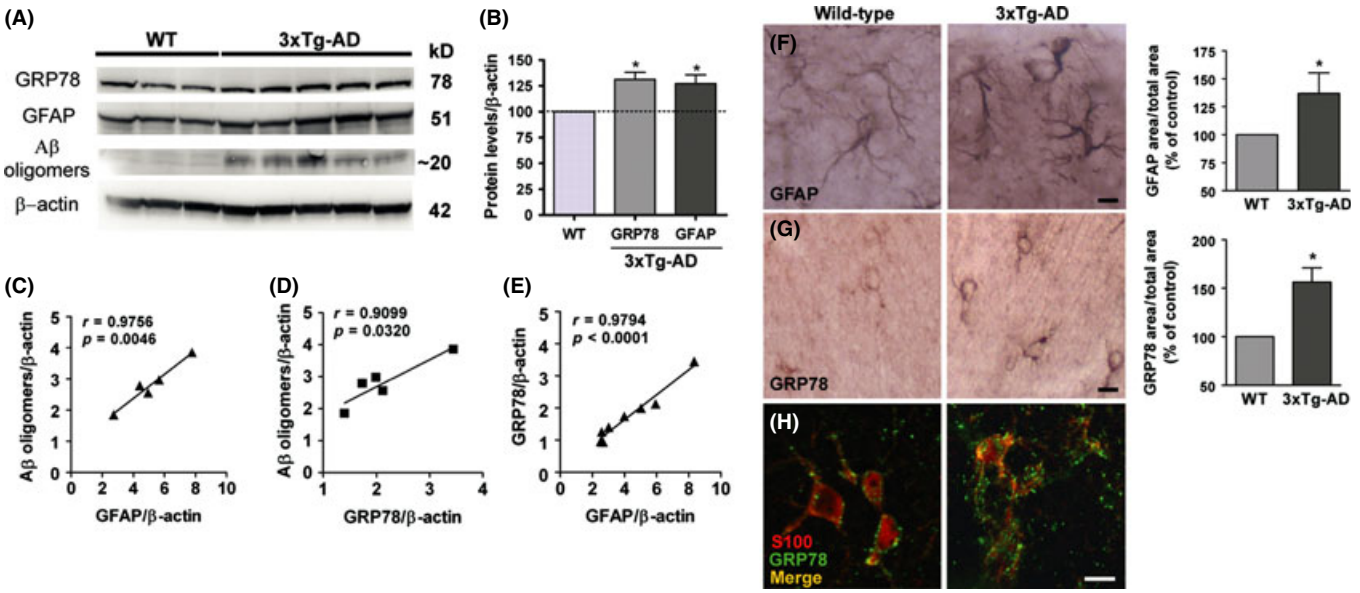


**Fig. 6** Oligomeric Aβ levels correlated with GFAP and GRP78 in the hippocampi of 3×Tg-AD mice. (A) Protein levels of GRP78, GFAP, and oligomeric Aβ in 12-month-old wild-type (WT; $n = 3$), and 3×Tg-AD mice ($n = 5$) were analyzed by Western blot. (B) Data represent optical density values of proteins normalized to β-actin values, expressed as a percentage of control values (100%). (C–E) Correlation analyses show significant positive correlations of Aβ oligomer levels with GFAP (C) or GRP78 (D) and between GRP78 and GFAP (E). (F–H) Photomicrographs of coronal sections of hippocampi of 12-month-old wild-type and 3×Tg-AD mice ($n = 6$ each group) show increased levels of GFAP (F) and GRP78 (G) in astrocytes of 3×Tg-AD mice compared with those of wild-type mice. (H) Photomicrographs of GRP78 revealed by double immunofluorescence labeling in S100-$B^+$ mouse astrocytes. Bar = 10 μm. *$P < 0.05$ compared with wild-type mice.

### ER $Ca^{2+}$ release and GFAP expression in amyloid β-treated astrocytes

Pathological insults to the CNS trigger reactive astrogliosis (Verkhratsky *et al.*, 2012). Astrogliosis by itself alters synaptic transmission and network excitability in the absence of neuronal pathology and microglial reactivity (Ortinski *et al.*, 2010). Therefore, pathological remodeling of astroglia associated with AD progression may directly contribute to neuronal signaling deficits (Olabarria *et al.*, 2010), and it is important to understand the mechanisms that stimulate astrocytes to acquire the reactive phenotype in AD. In the present study, we found that amyloid β directly triggered astrogliosis in an ER $Ca^{2+}$-dependent manner and that these changes correlated with ER stress *in vitro* and *in vivo*. These effects may impair a variety of astrocytic functions, including $Ca^{2+}$ signaling, expression of membrane transporters, secretion of neuroactive compounds, and morphological plasticity, which are central to glial modulation of neuronal signaling. However, further *in vivo* experiments are necessary to understand the link between dysregulated $Ca^{2+}$ homeostasis, ER stress, and astrocytic reactivity in amyloid β-treated cells.

### GFAP and GRP78 upregulation correlates with amyloid β oligomer levels in 3×Tg-AD mice

Accumulation of amyloid β is one of the earliest known molecular events in AD. Oligomers appear to be relatively stable structures; SDS-resistant species have been isolated from postmortem human brains, cell lines, and animal models of AD (Oddo *et al.*, 2006). Brains from 3×Tg-AD mice accumulate amyloid β oligomers in an age-dependent manner. In the current study, we observed increased levels of GFAP and GRP78 in hippocampal astrocytes of 3×Tg-AD mice at 12 months of age. These GFAP and GRP78 levels correlated with the levels of oligomeric amyloid β peptide, suggesting that oligomeric species may play a causal role in astrogliosis in this AD mouse model.

Mutations in APP, presenilin 1 and presenilin 2 genes change amyloid β metabolism leading to an increase in total amyloid β, alteration of the amyloid β 42/40 ratio or its propensity to aggregate (Selkoe, 2001). Furthermore, amyloid β accumulation plays a role in tau pathology in the 3×Tg-AD mice (Oddo *et al.*, 2006). Therefore, the involvement of tau and presenilin as inducers of astrogliosis cannot be excluded in this AD mouse model, and further experiments will be necessary to assess the link between astrogliosis and mutations in these three genes in the 3×Tg-AD. Our current observations indicate that astrocytes are a target for oligomeric amyloid β and support the hypothesis that the astrocyte response may contribute to brain damage in AD.

In summary, our results indicate that, in astrocytes, the ER $Ca^{2+}$ release through RyRs and $InsP_3Rs$ contributes to amyloid β-induced $Ca^{2+}$ dysregulation, generation of ER and oxidative stress, and astroglial reactivity. Markers of altered astrocytic physiology were consistently overexpressed in the hippocampal formation in amyloid β-injected brains. In 3×Tg-AD mice, the astrogliotic and cellular stress response correlated with an increase in oligomeric amyloid β species in the hippocampus, which is in agreement with amyloid β plaque-associated astrocytic hypertrophy observed in the CA1 area of the hippocampus (Olabarria *et al.*, 2010). Understanding astrocyte dysfunction in AD may help to define the links between amyloid β and progressive decline in cognitive function. Based on our data, we propose that molecules that stabilize ER $Ca^{2+}$ homeostasis in

astrocytes could represent potential targets in developing therapeutic applications for AD.

## Experimental procedures

### Preparation of amyloid β peptides

Oligomeric and fibrillar amyloid β (Aβ1–42) was prepared as reported previously (Dahlgren *et al.*, 2002). Briefly, Aβ1–42 (ABX, Radeberg, Germany) was initially dissolved in hexafluoroisopropanol (HFIP, Sigma, St. Louis, MO, USA) to a concentration of 1 mM. For the aggregation protocol, the peptide was resuspended in dry dimethylsulfoxide (5 mM; Sigma). Hams F-12 (PromoCell, LabClinics, Barcelona, Spain) or HCl (10 mM) were added to adjust the final peptide concentration to 100 μM to obtain oligomers (4 °C for 24 h) or fibrils (37ºC for 24 h), respectively.

### Astrocyte-rich cell culture

Primary cultures of cerebral cortical astrocytes were prepared from newborn (P0–P2) Sprague-Dawley rats as described previously (McCarthy & de Vellis, 1980; supporting information). After 2 weeks, cells were trypsinized and astrocytes were plated onto PDL-coated, 12-mm glass coverslips (for $Ca^{2+}$ imaging and immunocytochemistry), or six-well plates (for Western blotting).

### Preparation of organotypic cultures

Organotypic slices were prepared according to the previously described method (Alberdi *et al.*, 2010). Slices of entorhinal cortex and hippocampus were treated with Aβ 100 nM for 4 days and were immunostained with polyclonal anti-GFAP antibody (1:100; Dako, Glostrup, Denmark), rabbit polyclonal S100 (1:100; Dako), and monoclonal anti-ER retention signal KDEL (Grp78, Grp 94) (1:100; Stressgen Bioreagents, Ann Arbor, MI, USA). Labeling was detected with fluorescent goat anti-rabbit or sheep anti-mouse secondary antibodies (Alexa Fluor 488 and 546, Invitrogen, Barcelona, Spain). GFAP levels were measured by fluorimetry with a Synergy-HT fluorimeter (Bio-Tek Instruments Inc., Beverly, MA, USA; excitation at 540, emission at 570 nm). The colocalization colormap application of Image J (National Institutes of Health, Bethesda, MD, USA) was used to calculate GRP78 and S100 protein colocalization. Distribution of normalized mean deviation product (nMDP) values (ranging from −1 to 1) was visualized with a color scale, with indexes below 0 represented by cold colors (exclusion) and indexes above 0 represented by hot colors (colocalization).

### $Ca^{2+}$ imaging

Intracellular $Ca^{2+}$ levels were determined according to the previously described method (Alberdi *et al.*, 2010; Data S1).

### Protein preparation and Western blot analysis

Astrocytes ($2.5 \times 10^5$) were exposed to Aβ oligomers for 1, 6, or 24 h. Antagonists or inhibitors were added 15 min before addition of the Aβ oligomers. Cells were pelleted by centrifugation and lysed in gel-loading buffer for GRP78 and peIF2α analysis and in RIPA with protease inhibitor cocktail (Complete, Mini EDTA-free tablets, Roche, Mannheim, Germany) for GFAP analysis. Tissues from mice and organotypic slices were homogenized with a douncer, and sonicated in 200 μL or 100 μL, respectively, of RIPA with a protease inhibitor cocktail. Homogenates were centrifuged at 4°C for 15 min at 12 000×*g*. Proteins (10–20 μg) were analyzed by Western blot with the following specific primary antibodies: monoclonal anti-GFAP (0.1 μg/ml; Chemicon, Millipore Ibérica, Madrid, Spain), polyclonal antibodies against the phosphorylated and unphosphorylated forms of eukaryotic initiation factor 2α (peIF2α and eIF2α, respectively) (1:1000; Cell Signaling Technology, Beverly, MA, USA); monoclonal antibody against the ER retention signal KDEL (Grp 78) (1:1000; Stressgen Bioreagents); monoclonal anti-Aβ antibody (6E10, 1:1000; Covance, Emeryville, CA, USA); and polyclonal anti-β-actin antibody (1:5000; Sigma). Membranes were incubated with horseradish peroxidase-conjugated secondary antibodies (1:5000; Cell Signaling Technology) and were developed with Super Signal West Dura or Super Signal West Femto (Pierce, Rockford, IL, USA). The protein bands were detected with a ChemiDoc™ XRS Imaging System (Bio-Rad, Hercules, CA, USA), and the band intensities were quantified by density using Quantity One® (Bio-Rad, Hercules, CA, USA) software.

### Immunocytochemistry

Cells on coverslips were incubated with Aβ for 24 h, washed in ice-cold PBS, and fixed for 15 min in 4% PFA. Cells were permeabilized in methanol at −20 °C, washed in PBS and then saturated for 1 h in 4% NGS in PBS with 0.1% Triton-X 100 (blocking solution). Cells were then incubated for 2 h with polyclonal anti-GFAP antibody (dilution 1:100; Dako) in blocking solution. After washing, the cultures were incubated in PBS plus 4% NGS with goat anti-rabbit secondary antibody conjugated to Alexa Fluor® 488 (Invitrogen) for 1 h at room temperature. Immunofluorescence was visualized with an Observer Z1, Zeiss inverted microscope (Oberkochen, Germany). Photographs were acquired with a high-resolution, digital, AxioCam HRc camera (Zeiss, Oberkochen, Germany), and AxioVision software.

### Experimental animals, tissue preparation, and immunohistochemistry

Rats were divided into two groups: One group ($n = 8$) received a 10-μL injection of vehicle (DMSO 17%, Ham's F-12 83%) and a second group ($n = 8$) received an injection of Aβ peptide oligomers (40 μg/rat i.c.v.; more details in supporting information). Tissues from rats or 12-month-old 3 × Tg-AD animals and the non-Tg controls; $n = 6$ each group were fixed and processed as described previously (Gottlieb *et al.*, 2006). Coronal vibratome sections (40–50 μm) of the dorsal hippocampus were collected and processed for immunoperoxidase and immunofluorescence histochemistry. The mouse monoclonal antibody against GFAP (1:1000; Chemicon, Millipore Ibérica, Madrid, Spain), rabbit polyclonal antibody against S100 (1:100 Dako), and monoclonal antibody against the ER

retention signal KDEL (Grp78) (1:100, Stressgen Bioreagents) were used to quantify protein levels in 3–6 hippocampal sections per animal, from the control and Aβ-injected rats and wild-type and 3 × Tg-AD mice. Stained sections were observed and photographed with a digital camera (AxioCam MRc5, Zeiss) and Olympus Optical Fluoview FV500 confocal microscopy (40× magnification). Quantification of GFAP and GRP78 levels in astrocytes was performed using the threshold application of ImageJ software, and values are expressed as the percentage of astrocytic labeled area versus total area analyzed.

### Measurement of intracellular reactive oxygen species

Astrocytes were exposed to Aβ oligomers alone or with antagonists or inhibitors, as indicated. Cells were loaded with 30 μM CM-$H_2$DCFDA (Invitrogen, Barcelona Spain) to assay ROS levels. Calcein-AM (1 μM) was used to quantify the number of cells within the reading field. Fluorescence was measured with a Synergy-HT fluorimeter (Bio-Tek Instruments Inc.).

### Statistical Analysis

Data are presented as mean ± SEM. Statistical analysis was carried out with the Student's *t*-test. In all instances, a value of $P < 0.05$ was considered to indicate significance.

## Acknowledgments

We thank Hazel Gómez, Silvia Martín and Saioa Marcos for technical assistance. This study was supported by CIBERNED and by grants from the Ministerio de Ciencia e Innovación, the Departamento de Sanidad del Gobierno Vasco, Ikerbasque, and the Universidad del País Vasco.

## References

Abeti R, Abramov AY, Duchen MR (2011) Beta-amyloid activates PARP causing astrocytic metabolic failure and neuronal death. *Brain* **134**, 1658–1672.

Abramov AY, Canevari L, Duchen MR (2003) Changes in intracellular calcium and glutathione in astrocytes as the primary mechanism of amyloid neurotoxicity. *J. Neurosci.* **23**, 5088–5095.

Abramov AY, Canevari L, Duchen MR (2004) β-amyloid peptides induce mitochondrial dysfunction and oxidative stress in astrocytes and death of neurons through activation of NADPH oxidase. *J. Neurosci.* **24**, 565–575.

Alberdi E, Sánchez-Gómez MV, Cavaliere F, Pérez-Samartín A, Zugaza JL, Trullas R, Domercq M, Matute C (2010) Amyloid β oligomers induce $Ca^{2+}$ dysregulation and neuronal death through activation of ionotropic glutamate receptors. *Cell Calcium* **47**, 264–272.

Araque A (2008) Astrocytes process synaptic information. *Neuron Glia Biol.* **4**, 3–10.

Bao F, Wicklund L, Lacor PN, Klein WL, Nordberg A, Marutle A (2012) Different β-amyloid oligomer assemblies in Alzheimer brains correlate with age of disease onset and impaired cholinergic activity. *Neurobiol. Aging* **33**, e1–e13.

Busche MA, Eichhoff G, Adelsberger H, Abramowski D, Wiederhold KH, Haass C, Staufenbiel M, Konnerth A, Garaschuk O (2008) Clusters of hyperactive neurons near amyloid plaques in a mouse model of Alzheimer's disease. *Science* **321**, 1686–1689.

Chafekar SM, Hoozemans JJ, Zwart R, Baas F, Scheper W (2007) Aβ 1–42 induces mild endoplasmic reticulum stress in an aggregation state-dependent manner. *Antioxid. Redox Signal.* **9**, 2245–2254.

Chow SK, Yu D, Macdonald CL, Buibas M, Silva GA (2010) Amyloid β-peptide directly induces spontaneous calcium transients, delayed intercellular calcium waves and gliosis in rat cortical astrocytes. *ASN Neuro* **2**, e00026.

Dahlgren KN, Manelli AM, Stine WB Jr, Baker LK, Krafft GA, LaDu MJ (2002) Oligomeric and fibrillar species of amyloid-beta peptides differentially affect neuronal viability. *J. Biol. Chem.* **277**, 32046–32053.

De Felice FG, Velasco PT, Lambert MP, Viola K, Fernandez SJ, Ferreira ST, Klein WL (2007) Aβ oligomers induce neuronal oxidative stress through an *N*-methyl-D-aspartate receptor-dependent mechanism that is blocked by the Alzheimer drug memantine. *J. Biol. Chem.* **282**, 11590–11601.

Demuro A, Mina E, Kayed R, Milton SC, Parker I, Glabe CG (2005) Calcium dysregulation and membrane disruption as a ubiquitous neurotoxic mechanism of soluble amyloid oligomers. *J. Biol. Chem.* **280**, 17294–17300.

Demuro A, Parker I, Stutzmann GE (2010) Calcium signaling and amyloid toxicity in Alzheimer disease. *J. Biol. Chem.* **285**, 12463–12468.

Fiacco TA, McCarthy KD (2006) Astrocyte calcium elevations: properties, propagation, and effects on brain signaling. *Glia* **54**, 676–690.

Garwood CJ, Pooler AM, Atherton J, Hanger DP, Noble W (2011) Astrocytes are important mediators of Aβ-induced neurotoxicity and tau phosphorylation in primary cultures. *Cell Death Dis.* **2**, e167.

Gottlieb M, Leal-Campanario R, Campos-Esparza MR, Sánchez-Gómez MV, Alberdi E, Arranz A, Delgado-García JM, Gruart A, Matute C (2006) Neuroprotection by two polyphenols following excitotoxicity and experimental ischemia. *Neurobiol. Dis.* **23**, 374–386.

Hicks JB, Lai Y, Sheng W, Yang X, Zhu D, Sun GY, Lee JC (2008) Amyloid-beta peptide induces temporal membrane biphasic changes in astrocytes through cytosolic phospholipase A2. *Biochim. Biophys. Acta* **1778**, 2512–2519.

Hoozemans JJ, van Haastert ES, Nijholt DA, Rozemuller AJ, Eikelenboom P, Scheper W (2009) The unfolded protein response is activated in pretangle neurons in Alzheimer's disease hippocampus. *Am. J. Pathol.* **174**, 1241–1251.

Kuchibhotla KV, Goldman ST, Lattarulo CR, Wu HY, Hyman BT, Bacskai BJ (2008) Aβ plaques lead to aberrant regulation of calcium homeostasis in vivo resulting in structural and functional disruption of neuronal networks. *Neuron* **59**, 214–225.

Kuchibhotla KV, Lattarulo CR, Hyman BT, Bacskai BJ (2009) Synchronous hyperactivity and intercellular calcium waves in astrocytes in Alzheimer mice. *Science* **323**, 1211–1215.

McCarthy KD, de Vellis J (1980) Preparation of separate astroglial and oligodendroglial cell cultures from rat cerebral tissue. *J. Cell Biol.* **85**, 890–902.

Meske V, Hamker U, Albert F, Ohm TG (1998) The effects of β/A4-amyloid and its fragments on calcium homeostasis, glial fibrillary acidic protein and S100β staining, morphology and survival of cultured hippocampal astrocytes. *Neuroscience* **85**, 1151–1160.

Nedergaard M, Rodriguez JJ, Verkhratsky A (2010) Glial calcium and diseases of the nervous system. *Cell Calcium* **47**, 140–149.

Oddo S, Caccamo A, Shepherd JD, Murphy MP, Golde TE, Kayed R, Metherate R, Mattson MP, Akbari Y, LaFerla FM (2003) Triple-transgenic model of Alzheimer's disease with plaques and tangles: intracellular Abeta and synaptic dysfunction. *Neuron* **39**, 409–421.

Oddo S, Caccamo A, Tran L, Lambert MP, Glabe CG, Klein WL, LaFerla FM (2006) Temporal profile of amyloid-β (Aβ) oligomerization in an in vivo model of Alzheimer disease: a link between Aβ and tau pathology. *J. Biol. Chem.* **281**, 1599–1604.

Olabarria M, Noristani HN, Verkhratsky A, Rodríguez JJ (2010) Concomitant astroglial atrophy and astrogliosis in a triple transgenic animal model of Alzheimer's disease. *Glia* **58**, 831–838.

Ortinski PI, Dong J, Mungenast A, Yue C, Takano H, Watson DJ, Haydon PG, Coulter DA (2010) Selective induction of astrocytic gliosis generates deficits in neuronal inhibition. *Nat. Neurosci.* **13**, 584–591.

Peuchen S, Clark JB, Duchen MR (1996) Mechanisms of intracellular calcium regulation in adult astrocytes. *Neuroscience* **71**, 871–883.

Resende R, Ferreiro E, Pereira C, Resende de Oliveira C (2008) Neurotoxic effect of oligomeric and fibrillar species of amyloid-β peptide 1–42: involvement of endoplasmic reticulum calcium release in oligomer-induced cell death. *Neuroscience* **155**, 725–737.

Ruiz A, Matute C, Alberdi E (2009) Endoplasmic reticulum calcium release through ryanodine and $IP_3$ receptors contributes to neuronal excitotoxicity. *Cell Calcium* **46**, 273–281.

Ruiz A, Matute C, Alberdi E (2010) Intracellular $Ca^{2+}$ release through ryanodine receptors contributes to AMPA receptor-mediated mitochondrial dysfunction and ER stress in oligodendrocytes. *Cell Death Dis.* **1**, e54.

Santos AN, Ewers M, Minthon L, Simm A, Silber RE, Blennow K, Prvulovic D, Hansson O, Hampel H (2012) Amyloid-β oligomers in cerebrospinal fluid are associated with cognitive decline in patients with Alzheimer's disease. *J. Alzheimers Dis.* **29**, 171–176.

Scheper W, Nijholt DA, Hoozemans JJ (2011) The unfolded protein response and proteostasis in Alzheimer disease: preferential activation of autophagy by endoplasmic reticulum stress. *Autophagy* **7**, 910–911.

Selkoe DJ (2001) Alzheimer's disease: genes, proteins and therapy. *Physiol. Rev.* **81**, 741–766.

Shankar GM, Bloodgood BL, Townsend M, Walsh DM, Selkoe DJ, Sabatini BL (2007) Natural oligomers of the Alzheimer amyloid-β protein induce reversible synapse loss by modulating an NMDA-type glutamate receptor-dependent signalling pathway. *J. Neurosci.* **27**, 2866–2875.

Stix B, Reiser G (1998) β-amyloid peptide 25–35 regulates basal and hormone-stimulated Ca2+ levels in cultured rat astrocytes. *Neurosci. Lett.* **243**, 121–124.

Tomiyama T, Matsuyama S, Iso H, Umeda T, Takuma H, Ohnishi K, Ishibashi K, Teraoka R, Sakama N, Yamashita T, Nishitsuji K, Ito K, Shimada H, Lambert MP, Klein WL, Mori HA (2010) A mouse model of amyloid β oligomers: their contribution to synaptic alteration, abnormal tau phosphorylation, glial activation, and neuronal loss in vivo. *J. Neurosci.* **30**, 4845–4856.

Verkhratsky A (2005) Physiology and pathophysiology of the calcium store in the endoplasmic reticulum of neurons. *Physiol. Rev.* **85**, 201–279.

Verkhratsky A, Kettenmann H (1996) Calcium signalling in glial cells. *Trends Neurosci.* **19**, 346–352.

Verkhratsky A, Petersen OH (2002) The endoplasmic reticulum as an integrating signalling organelle: from neuronal signalling to neuronal death. *Eur. J. Pharmacol.* **447**, 141–154.

Verkhratsky A, Sofroniew MV, Messing A, deLanerolle NC, Rempe D, Rodriguez JJ, Nedergaard M (2012) Neurological diseases as primary gliopathies: a reassessment of neurocentrism. *ASN Neuro* **4**, e00082.

Vincent AJ, Gasperini R, Foa L, Small DH (2010) Astrocytes in Alzheimer disease: emerging roles in calcium dysregulation and synaptic plasticity. *J. Alzheimers Dis.* **22**, 699–714.

## Supporting Information

Additional supporting information may be found in the online version of this article at the publisher's web-site.

**Data S1.** Material and methods.